Effect of $1,25(OH)_2D_3$ on transdifferentiation of rat renal tubular epithelial cells induced by high glucose

HONGTAO HU, SHEN XU, SHUANG HU, YUE GAO and HUA SHUI

Department of Nephrology, Zhongnan Hospital of Wuhan University, Wuhan, Hubei 430071, P.R. China

Received May 15, 2016; Accepted August 19, 2016

DOI: 10.3892/br.2016.800

Abstract. Deficiency in vitamin D and its active metabolite is a characteristic of chronic kidney diseases (CKDs). Previous studies have reported that 1α,25-dihydroxyvitamin D_3 [$1,25(OH)_2D_3$], the active form of vitamin D, can attenuate renal interstitial fibrosis. The present study aimed to explore the effect of $1,25(OH)_2D_3$ on the transdifferentiation of NRK-52E rat renal tubular epithelial cells (RTECs) induced by high glucose, as well as the expression of vitamin D receptor (VDR) and production of angiotensin (Ang) II. Western blot and reverse transcription-quantitative polymerase chain reaction (RT-qPCR) analyses were performed to detect the protein and mRNA expression of α-smooth muscle actin (α-SMA), E-cadherin and VDR. Furthermore, the production of Ang II was analyzed by enzyme-linked immunosorbent assay (ELISA). Treatment with high glucose decreased E-cadherin and VDR, while increasing α-SMA and Ang II, and of note, these changes were attenuated by $1,25(OH)_2D_3$ in a dose-dependent manner. In conclusion, the present study revealed that $1,25(OH)_2D_3$ inhibits high glucose-induced transdifferentiation of rat RTECs in a dose-dependent manner, which may be associated with the downregulation of Ang II and upregulation of VDR.

Introduction

1α,25-dihydroxyvitamin D_3 [$1,25(OH)_2D_3$] has been originally known for its action on calcium and phosphorus homeostasis as well as bone mineralization. As a pleiotropic hormone with numerous regulatory effects, $1,25(OH)_2D_3$ has multiple physiological and pathological roles beyond the regulation of mineral metabolism, including the regulation of the immune system (1,2) and cardiovascular functions (3). The levels of vitamin D and 25-hydroxyvitamin D are significantly and inversely associated with blood pressure (4-6). Furthermore, emerging evidence for the important roles of vitamin D in the pathogenesis of metabolic disorders, such as obesity and diabetes, is accumulating (7). An increasing number of studies have shown that low plasma vitamin D_3 levels are an independent risk factor for a variety of cancer types, including colorectal (8,9), breast (10) and prostate cancer (11). Vitamin D_3 inhibits the proliferation and migration of a variety of cancer cell types, induce their differentiation and apoptosis, and has a potential anticancer effect (12,13).

Epithelial-mesenchymal transition (EMT) is a process by which epithelial cells are converted into mesenchymal cells. It occurs as part of several pathological processes, including tumor invasion and organ fibrosis, including renal fibrosis (7). Several studies have demonstrated the regulatory role of $1,25(OH)_2D_3$ in renal EMT (14-18). $1,25(OH)_2D_3$ was found to inhibit EMT via inducing a variety of target genes that encode cell adhesion and polarity proteins responsible for the epithelial phenotype, as well as through the repression of key EMT inducers (14). In renal tubulointerstitial fibrosis (RTF), EMT is known to represent the pathological basis of renal interstitial fibrosis characterized by downregulation of E-cadherin and upregulation of α-smooth muscle actin (α-SMA). In a mouse model of chronic kidney disease (CKD), unilateral ureteral obstruction (UUO)-induced RTF was ameliorated by administration of $1,25(OH)_2D_3$ (15). Other studies have found that $1,25(OH)_2D_3$ can attenuate the progression of renal interstitial fibrosis via inhibiting transforming growth factor (TGF)-β and high glucose-induced EMT (16-18). In the present study, the effects of $1,25(OH)_2D_3$ on the EMT of NRK-52E rat proximal tubular epithelial cell line induced by high glucose were investigated. Furthermore, the effects on the expression of vitamin D receptor (VDR) and angiotensin (Ang) II were assessed with the aim to explore the possible underlying mechanisms and to provide novel targets and strategies to delay the progress of renal interstitial fibrosis.

Materials and methods

Cell line and culture. The NRK-52E normal rat kidney epithelial cell line was purchased from the American Type Culture Collection (CRL-1571; Manassas, VA, USA). The NRK-52E cells were cultured in Dulbecco's modified Eagle's medium (low glucose; Gibco, Thermo Fisher Scientific, Inc., Waltham, MA, USA) containing 5% fetal bovine serum (FBS;

Correspondence to: Professor Hua Shui, Department of Nephrology, Zhongnan Hospital of Wuhan University, 169 Donghu Road, Wuhan, Hubei 430071, P.R. China
E-mail: shuihua2005@aliyun.com

Key words: 1α,25-dihydroxyvitamin D_3, epithelial-mesenchymal transition, NRK-52E, vitamin D receptor, angiotensin II

Gibco), 1% streptomycin (100 μg/ml) and penicillin (100 U/ml), and incubated in a humidified atmosphere containing 5% CO_2 at 37˚C. Upon reaching 90% confluency, the cells were passaged following detachment with 0.05% trypsin-ethylenediaminetetraacetate (Gibco), which was performed every 2 days.

Groups and treatments. One day prior to treatment, the NRK-52E cells were incubated with serum-free media for 24 h to synchronize the cell growth. The cells were randomly divided into the following five groups: control group (5.5 mmol/l glucose), high-glucose group (25 mmol/l glucose), high glucose with low dose of $1,25(OH)_2D_3$ group [25 mmol/l glucose with 10^{-9} mol/l $1,25(OH)_2D_3$], high glucose with a medium dose of $1,25(OH)_2D_3$ group [25 mmol/l glucose with 10^{-8} mol/l $1,25(OH)_2D_3$] and high glucose with a high dose of $1,25(OH)_2D_3$ group [25 mmol/l glucose with 10^{-7} mol/l $1,25(OH)_2D_3$]. Subsequent analyses were performed following for 24 h. Morphological observation was performed under a microscope (JS-500 binocular biological microscope; LIOO, Beijing, China) at x40 magnification before the cells were lysed.

Western blot analysis. Following washing in cold phosphate-buffered saline (PBS), the cells were lysed with radioimmunoprecipitation assay lysis buffer (Beyotime Institute of Biotechnology, Haimen, China) containing protease and phosphatase inhibitor (both from Roche, Mannheim, Germany). A Bradford Protein Assay (Beyotime Institute of Biotechnology) was performed to determine the total protein content. Twenty milligrams of total protein from each sample were separated by 12% sodium dodecyl sulfate-polyacrylamide gel electrophoresis and transferred onto a polyvinylidene difluoride membrane (Wuhan Boster Biological Technology, Ltd., Wuhan, China). Following incubation in 5% bovine serum albumin for 2 h at room temperature to block non-specific binding, the membranes were incubated overnight at 4˚C with primary antibodies against α-SMA (cat. no. ab32575; 1:2,000 dilution), E-cadherin (cat. no. ab76055; 1:1,000 dilution) or VDR (cat. no. ab109234; 1:1,000 dilution) (all from Abcam, Cambridge, MA, USA). Following three washes in Tris-buffered saline containing 0.1% Tween-20 for 10 min each, membranes were incubated with peroxidase-conjugated AffiniPure goat anti-rabbit immunoglobulin G (cat. no. 111035003; 1:10,000 dilution; Jackson ImmunoResearch Laboratories, Inc., West Grove, PA, USA) secondary antibody for at least 1 h at room temperature. Blots were visualized using an Enhanced Chemiluminescence Western Blotting Detection System (GE Healthcare Life Sciences, Chalfont, UK). The membrane was re-blotted with a rabbit anti-rat β-actin monoclonal antibody (cat. no. 4970; 1:1,000 dilution; Cell Signaling Technology, Inc.) to verify equal protein loading in each lane.

Reverse transcription-quantitative polymerase chain reaction (RT-qPCR). Total RNA from NRK-52E cells was extracted using TRIzol reagent (Invitrogen, Thermo Fisher Scientific, Inc.) according to the manufacturer's instructions. After determining the purity and quality of the total RNA, E-cadherin, α-SMA and VDR mRNA were quantified by RT-qPCR using the QuantiTect Reverse Transcription kit and the RNA SYBR-Green kit (both from Qiagen, Inc., Valencia, CA, USA) according to the manufacturer's instructions. PCR amplification was performed using the ABI 7500 Fast Real-Time PCR System (Applied Biosystems, Thermo Fisher Scientific, Inc.). The amplification program was 95˚C for 15 min followed by 40 cycles consisting of 95˚C for 10 sec and 60˚C for 35 sec. The ABI PRISM 7900HT Sequence Detection System (Applied Biosystems) was used to analyze the data, and the ΔΔCq method was used to calculate the relative expression of the respective sample gene (19). The sequences of the primers, which were designed using Primer Premier (v5.0; Premier Biosoft International, Palo Alto, CA, USA) based on the relevant sequences deposited in GenBank (http://www.ncbi.nlm.nih.gov/genbank/), are listed in Table I.

Table I. Primer sequences for polymerase chain reaction.

Gene		Sequence	Length (bp)
α-SMA	F	5'-CTGTTCCAGCCATCCTTCAT-3'	70
	R	5'-TCATGATGCTGTTGTAGGTGGT-3'	
E-cadherin	F	5'-CCAAAGCCTCAGGTCATTAAACA-3'	126
	R	5'-TTCTTGGGTTGGGTCGTTGTAC-3'	
VDR	F	5'-TGCTATGACCTGTGAAGGCT-3'	159
	R	5'-ATCATGCCGATGTCCACACA-3'	
GAPDH	F	5'-TGACATCAAGAAGGTGGTGA-3'	177
	R	5'-TCATACCAGGAAATGAGCTT-3'	

α-SMA, α-smooth muscle actin; F, forward; R, reverse; VDR, vitamin D receptor; GAPDH, glyceraldehyde-3-phosphate dehydrogenase.

Enzyme-linked immunosorbent assay (ELISA). The Ang II secreted into the culture supernatant by NRK-52E cells was detected by ELISA. The culture supernatant was collected and centrifuged at 8,000-12,000 x g for 20 min. ELISA plates (Nalge Nunc International, Thermo Fisher Scientific, Inc.) were coated with anti-Ang II monoclonal antibody (MoAb; Ziker Biological Technology, Ltd., Shenzhen, China) according to the instructions of the Rat Ang II ELISA kit (100 μl of a 10 μg/ml solution in 0.07 M NaCl buffered with 0.1 M borate, pH 8.2) and left overnight at 4˚C, followed by four washes with 200 μl of wash solution per well (0.9% w/v NaCl containing 0.05% v/v Tween-20). Subsequent to blocking with 200 μl PBS containing bovine serum albumin (1.0% w/v) and 0.05% v/v Tween-20 for 60 min at room temperature, wells were washed as described above. Centrifuged culture supernatant or serum samples (100 μl/well) were added, followed by incubation for 30 min at 37˚C. Subsequently, wells were incubated with horseradish peroxidase-conjugated streptavidin (1:4,000 dilution) for 30 min at 37˚C and tetramethylbenzidine (both from Zymed Laboratories, Inc., South San Francisco, CA, USA) as a substrate. The color reaction was allowed to develop for 30 min at 4˚C in the dark and was stopped by addition of 100 μl 0.2 M H_2SO_4 per well (Baker, Mexico City, Mexico). The optical density of each well at a wavelength of 450 nm (OD 450) was determined using an ELISA processor (Benchmark Microplate Reader; Bio-Rad Laboratories, Inc., Hercules, CA,

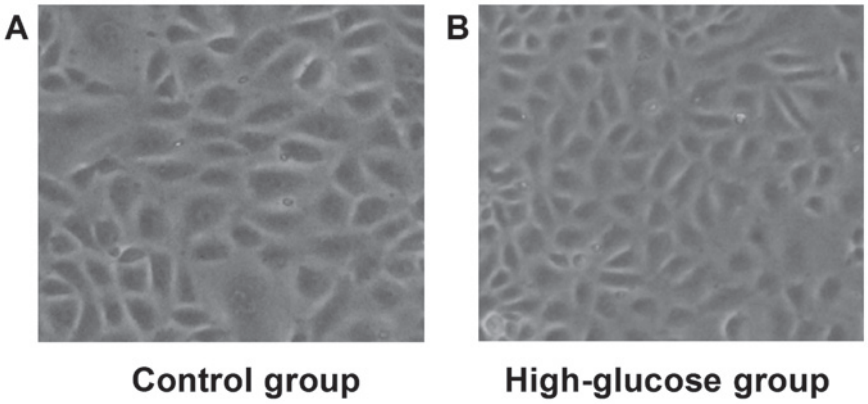

Figure 1. Effects of high glucose on cell morphology. Cells in the high-glucose group showed obvious transdifferentiation with cell polarity disappearing and morphology changing from (A) circular to (B) elliptic (magnification, x400).

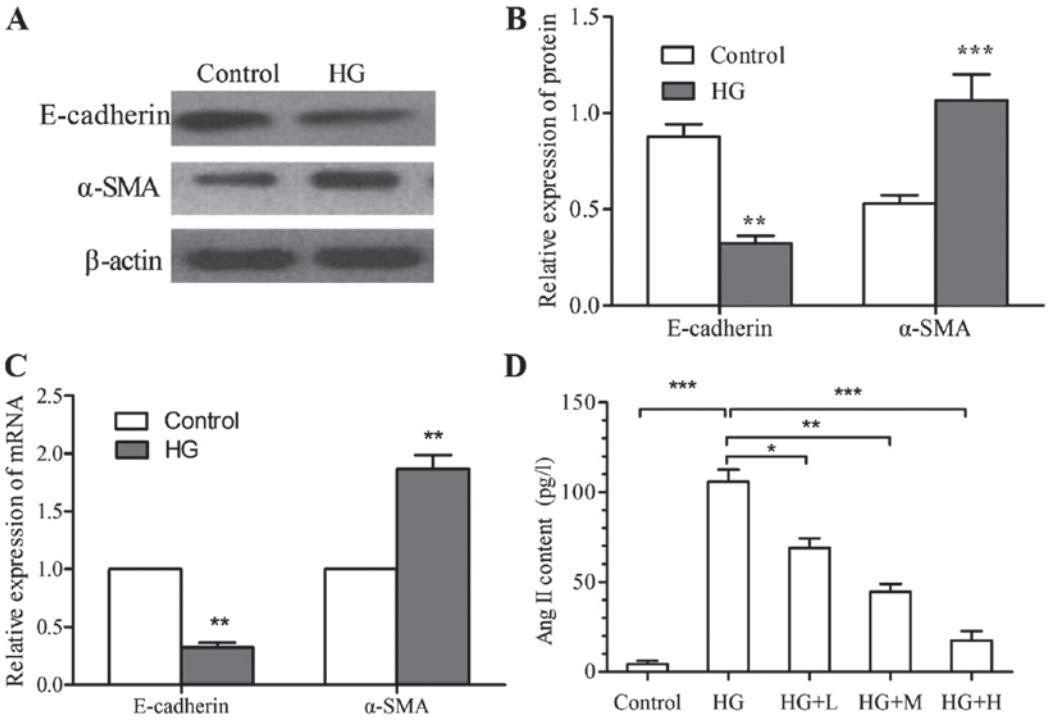

Figure 2. Effects of HG on the expression of molecular markers of the EMT transition and the secretion of Ang II. The expression of E-cadherin and α-SMA was assessed by (A and B) western blot analysis and (C) RT-qPCR analysis. (D) Ang II was detected in the culture supernatant by ELISA. Values are expressed as the mean ± standard deviation of results of experiments performed in triplicate. *P<0.05; **P<0.01; ***P<0.001 vs. control or as indicated. Groups: HG, high glucose (25 mmol/l); HG+L, high glucose with a low dose of $1,25(OH)_2D_3$ (10^{-9} mol/l); HG+M, high glucose with a medium dose of $1,25(OH)_2D_3$ (10^{-8} mol/l); HG+H, high glucose with a high dose of $1,25(OH)_2D_3$ (10^{-7} mol/l). HG, high glucose; EMT, epithelial-mesenchymal transition; Ang, angiotensin; α-SMA, α-smooth muscle actin; RT-qPCR, reverse transcription-quantitative polymerase chain reaction; ELISA, enzyme-linked immunosorbent assay; $1,25(OH)_2D_3$, 1α,25-dihydroxyvitamin D_3.

USA). The concentration of Ang II in the culture supernatant was determined from the OD 450 using a standard curve and the experiments were performed in triplicate.

Statistical analysis. Values are expressed as the mean ± standard deviation of results of experiments performed in triplicate. Statistical analysis was performed using SPSS 20.0 software (International Business Machines Corp., Armonk, NY, USA). The mean values were analyzed for their normality by using the Shapiro-Wilk normality test. All data passed the normality test and were tested for significant differences by one-way analysis of variance or Student's t-test. P<0.05 was considered to indicate a statistically significant difference between values. Each experiment was repeated three times.

Results

High glucose induces morphological changes of kidney cells characteristic of EMT. Initially, the effects of high glucose on the morphology of NRK-52E cells were assessed, which were observed by light microscopy following incubation with high glucose (25 mmol/l) for 24 h (Fig. 1). Compared to the control cells, those in the high-glucose group showed obvious trans-differentiation with cell polarity disappearing and the shape

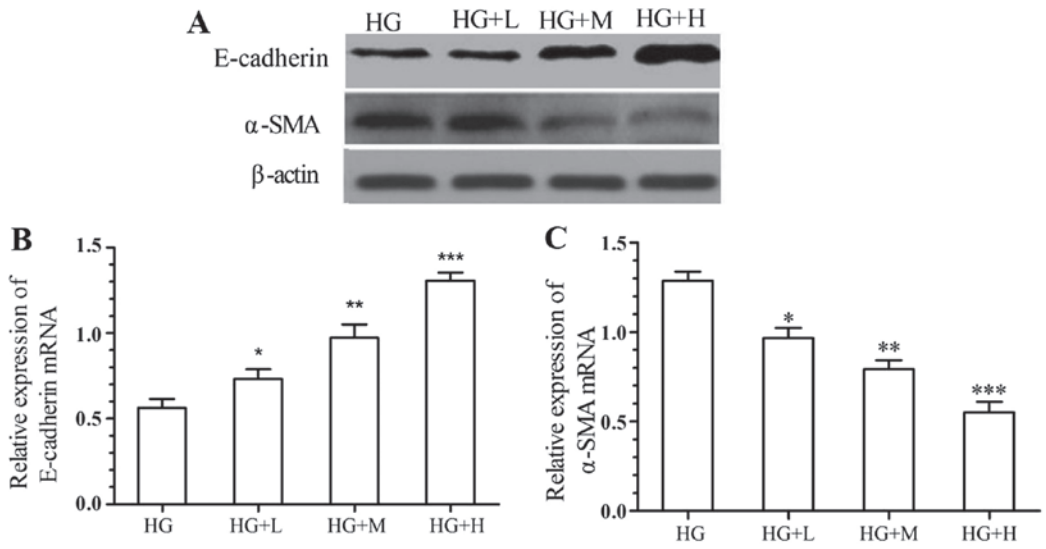

Figure 3. Inhibitory effects of 1,25(OH)$_2$D$_3$ on molecular markers of the EMT. The expression of E-cadherin and α-SMA was assessed by (A) western blot analysis and (B and C) RT-qPCR analysis. Values are expressed as the mean ± standard deviation of results of experiments performed in triplicate. *P<0.05; **P<0.01; ***P<0.001 vs. HG group. Groups: HG, high glucose (25 mmol/l); HG+L, high glucose with a low dose of 1,25(OH)$_2$D$_3$ (10^{-9} mol/l); HG+M, high glucose with a medium dose of 1,25(OH)$_2$D$_3$ (10^{-8} mol/l); HG+H, high glucose with a high dose of 1,25(OH)$_2$D$_3$ (10^{-7} mol/l). 1,25(OH)$_2$D$_3$, 1α,25-dihydroxyvitamin D$_3$; EMT, epithelial-mesenchymal transition; α-SMA, α-smooth muscle actin; RT-qPCR, reverse transcription-quantitative polymerase chain reaction; HG, high glucose.

changing from circular to elliptic, suggesting that high glucose can induce cell morphological changes associated with EMT.

High glucose induces expression of EMT-associated molecular markers and the secretion of Ang II by kidney cells. As high-glucose treatment resulted in cell morphological changes indicative of EMT, changes in the expression of molecular markers associated with epithelial and mesenchymal phenotypes by NRK-52E cells following high-glucose treatment were assessed. As determined by RT-qPCR and western blot analyses, respectively, the mRNA and protein levels of E-cadherin were significantly increased, while those of α-SMA were significantly reduced following high-glucose treatment (P<0.01) (Fig. 2A-C). Furthermore, ELISA revealed that the Ang II content in the culture supernatant of the high-glucose group (105.9±6.6 pg/l) was significantly higher than that in the control group (4.3±1.8 pg/l; P<0.001) (Fig. 2D).

1,25(OH)$_2$D$_3$ abrogates high glucose-induced EMT of kidney cells. In order to assess the inhibitory effects of 1,25(OH)$_2$D$_3$ on the EMT of kidney cells, the mRNA and protein expression of α-SMA and E-cadherin by NRK-52E cells was detected after incubation with various concentrations of 1,25(OH)$_2$D$_3$ and high glucose. As shown in Fig. 3, the high glucose-mediated reduction of E-cadherin in NRK-52E cells was significantly and dose-dependently attenuated by treatment with 1,25(OH)$_2$D$_3$. Furthermore, 1,25(OH)$_2$D$_3$ suppressed the high glucose-induced expression of α-SMA in a dose-dependent manner.

Effects of 1,25(OH)$_2$D$_3$ on the expression of VDR and Ang II. To further investigate the mechanisms by which 1,25(OH)$_2$D$_3$ inhibits high glucose-induced EMT, the mRNA and protein expression of VDR was analyzed using RT-qPCR and western blot analysis, while Ang II was detected by ELISA. The results showed that VDR expression was significantly downregulated

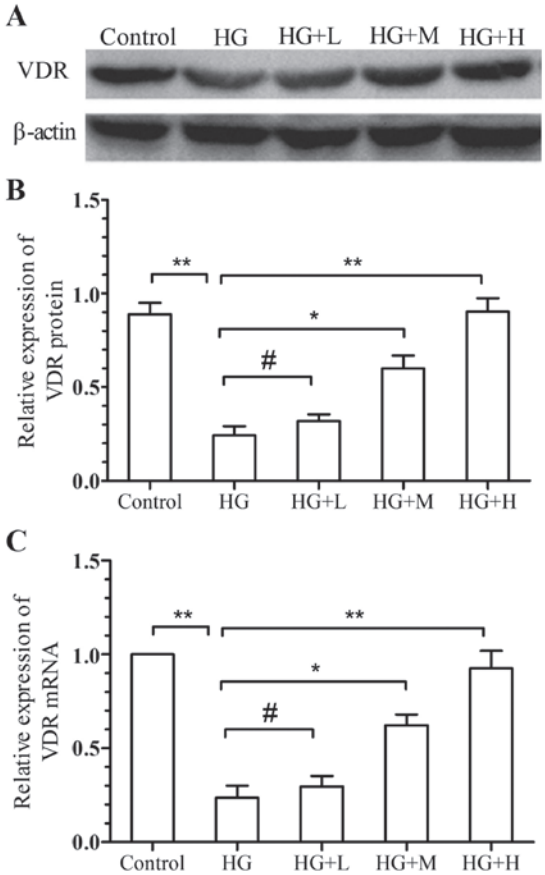

Figure 4. Effects of 1,25(OH)$_2$D$_3$ on the expression of VDR. The expression of VDR was assessed by (A and B) western blot analysis and (C) RT-qPCR analysis. Values are expressed as the mean ± standard deviation of results of experiments performed in triplicate. $^{\#}$P>0.05; *P<0.05, **P<0.01 vs. HG group. Groups: HG, high glucose (25 mmol/l); HG+L, high glucose with a low dose of 1,25(OH)$_2$D$_3$ (10^{-9} mol/l); HG+M, high glucose with a medium dose of 1,25(OH)$_2$D$_3$ (10^{-8} mol/l); HG+H, high glucose with a high dose of 1,25(OH)$_2$D$_3$ (10^{-7} mol/l). 1,25(OH)$_2$D$_3$, 1α,25-dihydroxyvitamin D$_3$; VDR, vitamin D receptor; RT-qPCR, reverse transcription-quantitative polymerase chain reaction; HG, high glucose.

by high-glucose stimulation, while $1,25(OH)_2D_3$ significantly inhibited this effect in a dose-dependent manner (Fig. 4). Furthermore, the Ang II content in the high-glucose group (105.9±6.6 pg/l) was significantly reduced by low, medium and high dose of $1,25(OH)_2D_3$ in a dose-dependent manner (68.9±5.5, 44.6±4.3 and 17.4±5.23 pg/l, respectively) $P<0.001$ (Fig. 2D).

Discussion

$1,25(OH)_2D_3$, the most active vitamin D_3 metabolite, is generated by its initial hydroxylation in the liver and subsequently in the kidney and other tissues. Within the last two decades, the endocrine and paracrine effects of vitamin D have been widely recognized. $1,25(OH)_2D_3$ has also gained attention for its cytoprotective effects in the kidney, and has been indicated to be important for maintaining podocyte health, preventing EMT transformation and suppressing the expression of renin as well as inflammation. Tian *et al* (20) revealed that vitamin D_3 exerts protective effects on the kidney in a rat model of diabetic nephropathy, probably by downregulating the expression of inflammatory factors, including TGF-β1, connective tissue growth factor and monocyte chemoattractant protein-1. Maquigussa *et al* (21) indicated that calcitriol supplementation may be a strategy to reduce renal damage induced by proteinuria in kidney disease. A number of studies have demonstrated the protective effects of $1,25(OH)_2D_3$ on the kidneys (18,20-22). In the present study, treatment of NRK-52E cells with high glucose for 24 h led to cell-morphological changes resulting in elliptic shapes, decreases of expression E-cadherin and increases of a-SMA expression, suggesting that the rat renal tubular cells underwent EMT. Simultaneously, addition of $1,25(OH)_2D_3$ inhibited high glucose-induced downregulation of E-cadherin and upregulation of α-SMA in a dose-dependent manner. These results provided evidence at the molecular level that $1,25(OH)_2D_3$ inhibits high glucose-induced EMT.

VDR, a member of the superfamily of nuclear receptors, is expressed in various kidney cell types, including proximal and distal tubular epithelial cells, glomerular parietal epithelial cells and collecting duct cells (23). VDR exerts multiple physiological and pathological functions by modulating the transcription of vitamin D-regulated genes via binding to vitamin D-responsive element. In a mouse model of UUO to simulate early CKD, the expression of VDR was significantly decreased, which was likely to be mediated by pro-inflammatory TNF-α, and late administration of active vitamin D was effective in restoring VDR expression (24). Wang *et al* (18) found that VDR(-/-) mice developed severe renal fibrosis following UUO, while $1,25(OH)_2D_3$ suppressed high glucose-induced apoptosis of podocytes. Ito *et al* (16) provided strong evidence that VDR suppresses renal fibrosis by inhibiting TGF-β-SMAD signal transduction. All of these studies, confirmed the critical role of $1,25(OH)_2D_3$-VDR signaling in renal protection. In the present study, high-glucose stimulation reduced the mRNA and protein expression of VDR in NRK-52E cells, which was dose-dependently inhibited by $1,25(OH)_2D_3$.

The renin-angiotensin-aldosterone system (RAAS) is a regulatory cascade with Ang II as the central effector. Dysregulation of the RAAS has a critical role in the pathogenesis of CKD. Diabetic kidney disease is the leading cause of CKD and blockade of the RAAS slows their progression to end-stage renal disease (25). Zhang *et al* (26) demonstrated that inhibition of Ang II activity with losartan reduced the development of renal fibrosis in mice subjected to UUO. In the present study, overproduction of Ang II was found in NRK-52E cells which underwent high glucose-induced EMT, which was inhibited by $1,25(OH)_2D_3$ in a dose-dependent manner. Of note, a previous study demonstrated that the inhibitory function of $1,25(OH)_2D_3$ on Ang II production was almost completely abrogated after silencing of the VDR gene (17). It is speculated that VDR inactivation leads to activation of the RAAS and that overproduction of Ang II and RAAS can be blocked by vitamin D/VDR signaling to attenuate renal fibrosis. The major mechanisms underlying the negative modulation of the RAAS by $1,25(OH)_2D_3$ appears to be: i) Suppression of renin gene transcription by blocking the activity of the cyclic adenosine monophosphate response element in the renin gene promoter (27); and ii) suppression of high glucose-induced angiotensinogen expression in kidney cells by blocking the nuclear factor-κB pathway (28).

In conclusion, the present study showed that $1,25(OH)_2D_3$ inhibits the transdifferentiation of rat renal tubular epithelial cells (RTECs) induced by high glucose in a dose-dependent manner, which may be associated with the inhibition of high glucose-induced upregulation of Ang II and downregulation of VDR. These results provided an experimental basis for further exploring the mechanisms of the renoprotective effects of $1,25(OH)_2D_3$ as well as a novel approach for the clinical treatment of renal fibrosis.

References

1. Baeke F, van Etten E, Gysemans C, Overbergh L and Mathieu C: Vitamin D signaling in immune-mediated disorders: Evolving insights and therapeutic opportunities. Mol Aspects Med 29: 376-387, 2008.
2. Kikuta J and Ishii M: Current topics on Vitamin D. The effects of vitamin D on the immune system. Clin Calcium 25: 359-365, 2015 (In Japanese).
3. Verstuyf A, Carmeliet G, Bouillon R and Mathieu C: Vitamin D: A pleiotropic hormone. Kidney Int 78: 140-145, 2010.
4. Afzal S and Nordestgaard BG: Low vitamin D and hypertension: A causal association? Lancet Diabetes Endocrinol 2: 682-684, 2014.
5. Schmitz KJ, Skinner HG, Bautista LE, Fingerlin TE, Langefeld CD, Hicks PJ, Haffner SM, Bryer-Ash M, Wagenknecht LE, Bowden DW, *et al*: Association of 25-hydroxyvitamin D with blood pressure in predominantly 25-hydroxyvitamin D deficient Hispanic and African Americans. Am J Hypertens 22: 867-870, 2009.
6. Margolis KL, Ray RM, Van Horn L, Manson JE, Allison MA, Black HR, Beresford SA, Connelly SA, Curb JD, Grimm RH Jr, *et al*; Women's Health Initiative Investigators: Effect of calcium and vitamin D supplementation on blood pressure: The Women's Health Initiative Randomized Trial. Hypertension 52: 847-855, 2008.
7. Nakashima A, Yokoyama K, Yokoo T and Urashima M: Role of vitamin D in diabetes mellitus and chronic kidney disease. World J Diabetes 7: 89-100, 2016.
8. Yin L, Grandi N, Raum E, Haug U, Arndt V and Brenner H: Meta-analysis: Longitudinal studies of serum vitamin D and colorectal cancer risk. Aliment Pharmacol Ther 30: 113-125, 2009.
9. Baron JA, Barry EL, Mott LA, Rees JR, Sandler RS, Snover DC, Bostick RM, Ivanova A, Cole BF, Ahnen DJ, *et al*: A trial of calcium and vitamin D for the prevention of colorectal adenomas. N Engl J Med 373: 1519-1530, 2015.

10. Reimers LL, Crew KD, Bradshaw PT, Santella RM, Steck SE, Sirosh I, Terry MB, Hershman DL, Shane E, Cremers S, *et al*: Vitamin D-related gene polymorphisms, plasma 25-hydroxyvitamin D, and breast cancer risk. Cancer Causes Control 26: 187-203, 2015.
11. Shui IM, Mondul AM, Lindström S, Tsilidis KK, Travis RC, Gerke T, Albanes D, Mucci LA, Giovannucci E and Kraft P; Breast and Prostate Cancer Cohort Consortium Group: Circulating vitamin D, vitamin D-related genetic variation, and risk of fatal prostate cancer in the National Cancer Institute Breast and Prostate Cancer Cohort Consortium. Cancer 121: 1949-1956, 2015.
12. Deeb KK, Trump DL and Johnson CS: Vitamin D signalling pathways in cancer: Potential for anticancer therapeutics. Nat Rev Cancer 7: 684-700, 2007.
13. Leyssens C, Verlinden L and Verstuyf A: Antineoplastic effects of $1,25(OH)_2D_3$ and its analogs in breast, prostate and colorectal cancer. Endocr Relat Cancer 20: R31-R47, 2013.
14. Larriba MJ, García de Herreros A and Muñoz A: Vitamin D and the epithelial to mesenchymal transition. Stem Cells Int 2016: 6213872, 2016.
15. Sun Y, Zhou G, Gui T, Shimokado A, Nakanishi M, Oikawa K, Sato F and Muragaki Y: Elevated serum $1,25(OH)_2$-vitamin D_3 level attenuates renal tubulointerstitial fibrosis induced by unilateral ureteral obstruction in kl/kl mice. Sci Rep 4: 6563, 2014.
16. Ito I, Waku T, Aoki M, Abe R, Nagai Y, Watanabe T, Nakajima Y, Ohkido I, Yokoyama K, Miyachi H, *et al*: A nonclassical vitamin D receptor pathway suppresses renal fibrosis. J Clin Invest 123: 4579-4594, 2013.
17. Gao P, Liu Y, Lin M, Chen YM, Shui H, Yao T and Wu XY: Effects of $1,25$-$(OH)_2D_3$ on the expression of vitamin D receptor and angiotensin IIII in human proximal tubular epithelial cells induced by high glucose. Chin J Diab 5: 495-499, 2013.
18. Wang Y, Deb DK, Zhang Z, Sun T, Liu W, Yoon D, Kong J, Chen Y, Chang A and Li YC: Vitamin D receptor signaling in podocytes protects against diabetic nephropathy. J Am Soc Nephrol 23: 1977-1986, 2012.
19. Livak KJ and Schmittgen TD: Analysis of relative gene expression data using real-time quantitative PCR and the 2(-Delta Delta C(T)) Method. Methods 25: 402-408, 2001.
20. Tian Y, Lv G, Yang Y, Zhang Y, Yu R, Zhu J, Xiao L and Zhu J: Effects of vitamin D on renal fibrosis in diabetic nephropathy model rats. Int J Clin Exp Pathol 7: 3028-3037, 2014.
21. Maquigussa E, Arnoni CP, Pereira LG and Boim MA: Calcitriol ameliorates renal damage in a pre-established proteinuria model. Mol Med Rep 12: 1009-1015, 2015.
22. Cozzolino M, Brunini F, Capone V, Ricca F, Kwaidri Y, Montanari E and Cusi D: Role of vitamin D in the pathogenesis of chronic kidney disease. Recenti Prog Med 104: 33-40, 2013 (In Italian).
23. Wang Y, Borchert ML and Deluca HF: Identification of the vitamin D receptor in various cells of the mouse kidney. Kidney Int 81: 993-1001, 2012.
24. Xiong M, Gong J, Liu Y, Xiang R and Tan X: Loss of vitamin D receptor in chronic kidney disease: A potential mechanism linking inflammation to epithelial-to-mesenchymal transition. Am J Physiol Renal Physiol 303: F1107-F1115, 2012.
25. Gurley SB and Coffman TM: The renin-angiotensin system and diabetic nephropathy. Semin Nephrol 27: 144-152, 2007.
26. Zhang Y, Kong J, Deb DK, Chang A and Li YC: Vitamin D receptor attenuates renal fibrosis by suppressing the renin-angiotensin system. J Am Soc Nephrol 21: 966-973, 2010.
27. Yuan W, Pan W, Kong J, Zheng W, Szeto FL, Wong KE, Cohen R, Klopot A, Zhang Z and Li YC: 1,25-dihydroxyvitamin D_3 suppresses renin gene transcription by blocking the activity of the cyclic AMP response element in the renin gene promoter. J Biol Chem 282: 29821-29830, 2007.
28. Deb DK, Chen Y, Zhang Z, Zhang Y, Szeto FL, Wong KE, Kong J and Li YC: 1,25-Dihydroxyvitamin D_3 suppresses high glucose-induced angiotensinogen expression in kidney cells by blocking the NF-κB pathway. Am J Physiol Renal Physiol 296: F1212-F1218, 2009.